Space Frame Optimization Subject to Frequency Constraints

Tze Hsin Woo*
TRW Space and Technology Group, Redondo Beach, California

An efficient structural optimization methodology is presented for the design of minimum-weight space frames subject to multiple natural frequency constraints. A powerful class of generalized hybrid constraint approximations that require only the first-order constraint function derivatives has been developed to overcome the inherent nonlinearity of the frequency constraint. The generalized hybrid constraint functions are shown to be relatively conservative, separable, and convex in the region bounded by the move limits based on the formula described in this paper. The optimization methodology is implemented in an automated structural optimization system, which has been applied to solve a variety of space frame optimization problems. Numerical results obtained for three example problems indicate that the optimization methodology requires fewer than 10 complete normal modes analyses to generate a near-optimum solution.

Nomenclature

A = cross-sectional area
B = cross-sectional width
$\boldsymbol{b}$ = constant vector
C = constant matrix
$\boldsymbol{d}$ = vector of design variables before basis reduction
E = Young's modulus
g_j = jth constraint function
$\tilde{g}_j$ = jth approximate constraint function
$\tilde{g}_{\mathrm{GHC}j}$ = jth generalized hybrid constraint function
H = cross-sectional depth
I = upper limit on index i
J = upper limit on index j
K = global stiffness matrix
M = global mass matrix
m = nonstructural mass
R = mean radius of thin-wall round tube
t = thickness
w = objective function (structural weight)
X, Y, Z = Cartesian coordinates
$\boldsymbol{x}$ = vector of independent design variables
α_{ij} = convolution function for ith design variable and jth constraint
λ_j = jth eigenvalue
$\boldsymbol{\phi}_j$ = jth eigenvector
υ = Poisson's ratio
ρ = material density
ω_j = jth natural frequency

Superscripts

ℓ = lower-bound quantities
T = transpose of a matrix
u = upper-bound quantities

I. Introduction

STRUCTURAL optimization of three-dimensional space frame type structures has made considerable progress in recent years. The majority of the reported research effort and computational experience has focused on the space frame optimization subject to static constraints.[1-4] There is, however, a significant class of structural design optimization problems in which limits are placed on the natural vibration frequencies and structural models involving beam elements. For example, in spacecraft design, frequency requirements are imposed as preliminary measures to prevent excessive dynamic structural responses and to avoid coupling between the structure and control system. In structural analysis, a significant portion of the spacecraft structure is modeled with beam elements to capture the essential structural behavior without an inordinate computational burden.

A number of methods have been proposed for the structural optimization subject to a single frequency constraint.[5-8] These methods were developed for simple beams and two-dimensional truss-membrane type structures. Their application to three-dimensional frame structures has not been successful. By combining mathematical programming techniques, finite-element structural analysis, and some approximation concepts, Miura and Schmit studied optimization problems with a frequency constraint for two- and three-dimensional truss membrane structures.[9] They reported that, due to the inherent nonlinearity of natural frequency constraints, a second-order Taylor series approximation for each eigenvalue of the equation of motion may be needed to improve the stability and overall efficiency of the optimization process. However, the computation of the second-order eigenvalue derivatives is very tedious and expensive. The heavy computational burden in the optimization process is shifted, but preserved, from a large number of costly normal modes analyses using the first-order Taylor series approximation to very expensive calculations of the Hessian matrices required in the second-order Taylor series. The difficulty of nonlinearity is further compounded in the space frame optimization subject to frequency constraints because each beam element may have multiple design variables, and functional relations between section properties and design variables for the beam element are much more complicated than those for the truss and membrane elements. Unless a simple, high-quality frequency constraint approximation is found, the solution of practical structural optimization problems may not be computationally feasible.

This paper reports an efficient methodology that requires fewer than 10 normal modes analyses to generate a near-optimum solution for the space frame optimization problems with multiple frequency constraints. The methodology is based on the finite-element analysis, some approximation concepts, and nonlinear mathematical programming techniques. A class of generalized hybrid constraint approximations which require only the first-order derivatives of the function to be approximated is developed to overcome the

Presented as Paper 86-0877 at the AIAA/ASME/ASCE/AHS 27th Structures, Structural Dynamics and Materials Conference, San Antonio, TX, May 19-21, 1986; received April 18, 1986; revision received Nov. 19, 1986. Copyright © 1987 by T. H. Woo. Published by the American Institute of Aeronautics and Astronautics, Inc., with permission.

*Head, Methodology Development. Member AIAA.

difficulty of nonlinearity. A comprehensive cross-sectional library is established to handle functional relations between cross-sectional properties and design variables. A large-scale general-purpose computer software system is developed to implement the optimization method. Example problems and numerical results are presented in this paper to illustrate the effectiveness of the hybrid constraint approximation and the efficiency of the optimization methodology.

II. Optimization Problem

The space frame structural optimization problem may be stated as follows: seek a minimum-weight design such that the natural vibration frequencies and all structural design variables remain within specified limits. For the case where the structural topology, configuration, and materials are prescribed, the design optimization problem can be formulated as follows:

Minimize

$$w(\boldsymbol{d})$$

subject to

$$\lambda_j \le \lambda_j \le \lambda_j^u, \qquad [K-\lambda_j M]\boldsymbol{\phi}_j = 0$$

$$\lambda_j = \omega_j^2, \quad \boldsymbol{Cd}-\boldsymbol{b} \le 0, \quad \boldsymbol{d}^\ell \le \boldsymbol{d} \le \boldsymbol{d}^u; \qquad j=1,\ldots,J \tag{1}$$

where $\boldsymbol{Cd}-\boldsymbol{b}\le 0$ is a set of general linear constraints.

Problem (1) is a highly implicit, nonlinear, nonconvex problem for which approximate solutions can be obtained, in principle, by mathematical programming methods. However, the direct solution of problem (1) is computationally impractical because a large number of eigenvalue problems have to be solved to obtain the natural frequencies and their derivatives required in the optimization process. A more tractable approach is to solve problem (1) as a sequence of explicit approximation problems of reduced dimensionality while preserving the essential features of the original problem.[9,10]

The number of independent design variables can be reduced by design variable linking, which in its simplest form fixes the relative sizes of a preselected set of design variables. The reduced basis concept in the design space can be used to further reduce the number of independent design variables by expressing the original vector of design variables as a linear combination of prelinked basis vectors. Let $x=[x_1,x_2,\ldots,x_I]^T$ be a design vector of reduced dimensionality, and the original design vector can be expressed as

$$\boldsymbol{d} = x_1\boldsymbol{d}^1 + x_2\boldsymbol{d}^2 + \ldots + x_I\boldsymbol{d}^I \tag{2}$$

where $\boldsymbol{d}^1$ through $\boldsymbol{d}^I$ are prelinked basis vectors. It is important to recognize that design variable linking and/or basis reduction represent essential features in practical design application because they facilitate the introduction of fabrication and cost control considerations as well as the designer's insight and prior experience.

The equality constraints in problem (1) can be eliminated when eigenvalues are approximated by explicit functions of the independent design variables. Let $\tilde{g}_j$ be an approximate eigenvalue constraint function and substitute Eq. (2) into problem (1); an approximate optimization problem can be written as

Minimize

$$w(\boldsymbol{x})$$

subject to

$$\tilde{g}_j(\boldsymbol{x}) \le 0, \qquad j=1,\ldots,2J$$

$$\sum_i \boldsymbol{C}x_i\boldsymbol{d}^i - \boldsymbol{b} \le 0$$

$$\boldsymbol{x}^\ell \le \boldsymbol{x} \le \boldsymbol{x}^u \tag{3}$$

where

$$\tilde{g}_j \cong g_j = \lambda_j^\ell - \lambda_j \tag{4a}$$

$$\tilde{g}_{J+j} \cong g_{J+j} = \lambda_j - \lambda_j^u \tag{4b}$$

A number of nonlinear programming algorithms can be used to obtain a solution for problem (3). However, if problem (3) is a good approximation to the original problem only within a small region of the design space, either a large number of approximate problems have to be solved to obtain a near-optimum solution, or the optimization process does not converge at all. Therefore, the quality of the frequency constraint approximation plays a key role in the successful development of an efficient structural optimization methodology.

III. Eigenvalue Derivatives

Various methods are available to construct constraint approximations. The majority of these methods require derivatives of the function to be approximated. In the case of the natural frequency constraints, the calculation of the constraint function derivatives requires partial derivatives of the eigenvalue with respect to independent design variables. The following expression for the first-order eigenvalue derivative was initially derived and presented by Fox and Kapoor.[11]

$$\frac{\partial\lambda_j}{\partial x_i} = \boldsymbol{\phi}_j^T\left(\frac{\partial K}{\partial x_i} - \lambda_j\frac{\partial M}{\partial x_i}\right)\boldsymbol{\phi}_j \tag{5}$$

$$\boldsymbol{\phi}^T M\boldsymbol{\phi} = 1 \tag{6}$$

The second-order eigenvalue derivatives which are required in the higher-order Taylor series approximation of the constraint function for truss-membrane type structures, were presented in Ref. 9. Since the stiffness and mass matrices are linear functions of the design variables, such as the truss member cross-sectional area and membrane thickness, some simplifications result in the expression for the second-order eigenvalue derivatives. This is not the case for space frame structures, because the stiffness and mass matrices are nonlinear functions of the design variables, such as cross-sectional dimensions. Using the derivation similar to that given in Ref. 9, the general expression for the second-order eigenvalue derivative can be written as

$$\frac{\partial^2\lambda_j}{\partial x_k\partial x_i} = F_{1j} + F_{2j} + F_{3j} \tag{7}$$

where

$$F_{1j} = \boldsymbol{\phi}_j^T\left(\frac{\partial^2 K}{\partial x_k\partial x_i} - \lambda_j\frac{\partial^2 M}{\partial x_k\partial x_i}\right)\boldsymbol{\phi}_j \tag{8}$$

$$F_{2j} = -\boldsymbol{\phi}_j^T\left(\frac{\partial\lambda_j}{\partial x_i}\frac{\partial M}{\partial x_k} + \frac{\partial\lambda_j}{\partial x_k}\frac{\partial M}{\partial x_i}\right)\boldsymbol{\phi}_j \tag{9}$$

$$F_{3j} = \boldsymbol{\phi}_j^T\left(\frac{\partial F_j}{\partial x_i}\frac{\partial\boldsymbol{\phi}_j}{\partial x_k} + \frac{\partial F_j}{\partial x_k}\frac{\partial\boldsymbol{\phi}_j}{\partial x_i}\right) \tag{10}$$

$$\frac{\partial F_j}{\partial x_i} = \frac{\partial K}{\partial x_i} - \frac{\partial\lambda_j}{\partial x_i}M - \lambda_j\frac{\partial M}{\partial x_i} \tag{11}$$

For truss membrane structures, F_{1j} vanishes. The influence of the first-order eigenvector derivatives on the second-order eigenvalue derivative is represented by F_{3j} in Eqs. (7) and (10). The computation of the eigenvector derivative is very tedious and expensive, even with the simplified procedure presented by Nelson,[12] because it requires a number of matrix multiplications and the solution of a set of simul-

taneous equations. A comparison between Eq. (5) and Eqs. (7-11) indicates that the computational burden for the second-order eigenvalue derivatives is much heavier than that required for the first-order derivatives.

IV. Generalized Hybrid Constraint Approximation

The most commonly used approximation techniques require only the first-order constraint function derivatives. The concept of reciprocal design variables was introduced by Schmit and Farshi[10] to improve the quality of the first-order Taylor series approximation. An innovative hybrid constraint approximation, which is more conservative than the linear Taylor series in either the design or the reciprocal design space, was presented by Starnes and Haftka.[13] A significant generalization of the hybrid constraint approximation based on the first-order Taylor series, the inverse power and logarithmic transformations of design variables was reported by Prasad.[14,15] No proof of relative conservativeness was given by Prasad for his general case of the hybrid constraint approximation. For a structural optimization problem involving different types of constraints, it may be difficult to find a set of design variable transformations that will yield a high-quality first-order Taylor series approximation for each constraint. For example, if nonlinear design variable transformations are used for the eigenvalue constraints, the general linear constraints in Eq. (1) will be nonlinearized by the transformations and then approximated by the first-order Taylor series.

It was reported[9] that the first-order Taylor series is a poor approximation for the frequency constraint, and a large number of normal modes analyses are required to obtain a near-optimum solution. It was also suggested[9] that the second-order Taylor series might be needed to provide a more accurate approximation of the eigenvalue constraint. Unfortunately, the calculation of th second-order eigenvalue derivatives and the first-order eigenvector derivatives imposes a heavy computational burden in the structural optimization process. To overcome this difficulty, the hybrid constraint approximation presented by Starnes and Haftka[13] is generalized, without using any design variable transformation, to handle the highly nonlinear eigenvalue constraints.

The first-order Taylor series approximation of a nonlinear constraint boundary represents a hyperplane in the design space. If the hyperplane can be deformed toward the interior of the feasible region, the resulting surface will be a more conservative constraint boundary approximation than the hyperplane. Furthermore, if an explicit expression can be found for the approximate constraint surface without using higher-order derivatives, the evaluation of the approximate constraint will be relatively simple. Based on these observations, a convoluted Taylor series is defined as follows:

$$\tilde{g}_j(\boldsymbol{x}) = g_j(\boldsymbol{x}_0) + \sum_{i=1}^{I} \frac{\partial g_j(\boldsymbol{x}_0)}{\partial x_i} (x_i - x_{i0}) \alpha_{ij}(x_i) \tag{12}$$

where α_{ij} is an explicit real function of the ith independent design variable x_i. It should be noted that $\tilde{g}_j$ in Eq. (12) is a separable function of the design variables and involves only the first-order derivatives of the constraint function. The convolution function α_{ij} plays a key role in the conservativeness of approximation given by Eq. (12). A simple and effective convolution function can be defined as

$$\alpha_{ij}(x_i) = (x_i/x_{i0})^{r_{ij}} \tag{13}$$

where r_{ij} is a real number. Substitute Eq. (13) into Eq. (12) to obtain the following:

$$\tilde{g}_j^r = g_j(\boldsymbol{x}_0) + \sum_{i=1}^{I} \frac{\partial g_j(\boldsymbol{x}_0)}{\partial x_i} (x_i - x_{i0})(x_i/x_{i0})^{r_{ij}} \tag{14}$$

If $r_{ij} = 0$, Eq. (14) becomes the first-order Taylor series approximation in the design space. If $r_{ij} = -1$, Eq. (14) is equivalent to the linear Taylor series expansion with respect to reciprocal design variables.

Let n_{ij} be a positive integer and p_{ij} be a real number. For $r_{ij} = p_{ij}$ and $r_{ij} = p_{ij} - n_{ij}$, a pair of approximate constraint functions, $\tilde{g}_j^p$ and $\tilde{g}_j^{p-n}$, can be generated from Eq. (14). With the understanding that the values of the parameters r, p, and n may be different for each constraint and each design variable, the subscripts i and j for the parameters r, p, and n will be dropped to simplify the notation:

$$\tilde{g}_j^p - \tilde{g}_j^{p-n} = \sum_{i=1}^{I} \frac{\partial g_j(\boldsymbol{x}_0)}{\partial x_i} (x_i - x_{i0})[(x_i/x_{i0})^p - (x_i/x_{i0})^{p-n}]$$

$$(x_i - x_{i0})[(x_i/x_{i0})^p - (x_i/x_{i0})^{p-n}] \tag{15}$$

$$= (x_i^{p-n}/x_{i0}^p)(x_i - x_{i0})(x_i^n - x_{i0}^n)$$

$$= (x_i^{p-n}/x_{i0}^p)(x_i - x_{i0})^2(x_i^{n-1} + x_i^{n-2}x_{i0} + \ldots + x_{i0}^{n-1}) \tag{16}$$

Without loss of generality, it is assumed that

$$x_i > 0, \qquad x_{i0} > 0, \qquad i = 1,\ldots,I \tag{17}$$

This means that the right-hand side of Eq. (16) is greater than or equal to zero:

$$(x_i - x_{i0})[(x_i/x_{i0})^p - (x_i/x_{i0})^{p-n}] \geq 0 \tag{18}$$

Using Eqs. (18) and (15), the following is obtained:

$$\tilde{g}_j^p - \tilde{g}_j^{p-n} \leq 0 \text{ if } \frac{\partial g_j(\boldsymbol{x}_0)}{\partial x_i} \geq 0 \text{ for all } i \tag{19}$$

$$\tilde{g}_j^p - \tilde{g}_j^{p-n} \leq 0 \text{ if } \frac{\partial g_j(\boldsymbol{x}_0)}{\partial x_i} \leq 0 \text{ for all } i \tag{20}$$

If Eq. (19) holds, $\tilde{g}_j^p$ is a more conservative approximation than $\tilde{g}_j^{p-n}$. If Eq. (20) is true, $\tilde{g}_j^{p-n}$ is more conservative than $\tilde{g}_j^p$. Unfortunately, the eigenvalue constraint function derivatives may not be all positive or all negative. A generalized hybrid constraint (GHC) approximation that is more conservative than either $\tilde{g}_j^p$ or $\tilde{g}_j^{p-n}$ can be defined as

$$\tilde{g}_{\mathrm{GHC}j}(\boldsymbol{x}) = g_j(\boldsymbol{x}_0) + \sum_{i=1}^{I} \frac{\partial g_j(\boldsymbol{x}_0)}{\partial x_i} f_{ij}(x_i) \leq 0 \tag{21}$$

$$f_{ij}(x_i) = (x_i - x_{i0})(x_i/x_{i0})^r \tag{22}$$

$$r = p \text{ if } \partial g_j(\boldsymbol{x}_0)/\partial x_i \geq 0, \qquad r = p - n \text{ if } \partial g_j(\boldsymbol{x}_0)/\partial x_i < 0 \tag{23}$$

The GHC approximation is a simple explicit approximation that requires only the first-order derivatives of the function to be approximated. It is efficient to use a GHC in a structural optimization process because the computational cost of a GHC is approximately the same as that required for the first-order Taylor series. The GHC with $p \geq 0$ and $p - n \leq -1$ is more conservative than the linear Taylor series approximation in either the design space or the reciprocal design space. Since the fundamental concept of the GHC is the deformation of the hyperplane represented by the linear Taylor series, in many cases the deformation captures some nonlinear characteristics of the constraint function and the GHC provides a better approximation than the linear Taylor series. The relative conservativeness of the GHC can be tuned by adjusting the parameters p and n. Larger values used for p and n will make the GHC more conservative. Since different values of p and n may be used for each con-

straint and each design variable, the general linear constraints in Eq. (1) will remain linear if $p=n=0$ is used for the linear constraints.

Convexity

The concept of convexity is of great importance in the analysis and solution of optimization problems. If an optimization problem is convex, the Kuhn-Tucker optimality condition becomes not only necessary but also sufficient, and the existence of a saddle point is guaranteed. The majority of structural optimization problems, including those subject to frequency constraints, are nonconvex. It is extremely difficult to theoretically prove, except for a class of plastic structural design optimization problems (see Ref. 16), that a solution of a structural optimization problem is a global optimum. Therefore, a near-optimum solution is considered to be acceptable in the optimization of complex structures.

Since the solution approach used here is to replace the original problem by a sequence of approximate problems, it is important to analyze the approximate problem and study its mathematical properties. The generalized hybrid constraint function defined in Eqs. (21-23) is a nonlinear separable function of design variables. It can be shown that a subclass of the GHC function is convex. Differentiating Eq. (22) twice obtains the following second derivative:

$$\frac{d^2 f_{ij}}{dx_i^2}=\frac{x_i^{r-2}}{x_{i0}^{r-1}}\left[(r+1)\frac{x_i}{x_{i0}}-(r-1)\right] \tag{24}$$

Under the assumption of Eq. (17), it is obvious that

$$\frac{d^2 f_{ij}}{dx_i^2}\begin{cases}\geq 0 \text{ if } 0\leq r\leq 1\\ <0 \text{ if } -1\leq r<0\end{cases} \tag{25}$$

which means that the function f_{ij} is convex if $0\leq r\leq 1$ and concave if $-1\leq r<0$. Since the negative of a concave function is convex and the positive linear combination of convex functions is convex, the GHC function is convex if $0\leq p\leq 1$ and $-1\leq p-n<0$.

For the case $r>1$

$$\frac{d^2 f_{ij}}{dx_i^2}\geq 0 \text{ if } \frac{x_i}{x_{i0}}\geq\frac{r-1}{r+1} \tag{26}$$

For the case $r<-1$

$$\frac{d^2 f_{ij}}{dx_i^2}\leq 0 \text{ if } \frac{x_i}{x_{i0}}\leq\frac{r-1}{r+1} \tag{27}$$

Equations (26) and (27) define the lower and upper bounds of the region in which the GHC function is convex. Combining Eqs. (25-27), it can be stated that the GHC function given by Eqs. (21-23) is separable and convex if

$$p\geq 0, \qquad p-n<0 \tag{28}$$

and

$$\frac{P-1}{P+1}\leq\frac{x_i}{x_{i0}}\leq\frac{p-n-1}{p-n+1} \text{ if } p>1, \quad p-n<-1 \tag{29}$$

Equation (29) can be viewed as move limits in the optimization process. The move limits given by Eq. (29) are usually quite generous. For example, if $p=3$ and $n=6$, the lower and upper move limits are 50 and 200%, respectively. It should be noted that the convexity proof is valid even if n is a real number.

The objective function in the optimization problem can also be approximated by a generalized hybrid function similar to the GHC function. The resulting approximate problem is separable and convex within the move limits defined by Eq. (29). A global optimum solution of the approximate problem can be obtained by nonlinear programming algorithms. In addition, since there is no duality gap between the primal and dual approximate problems, the dual method reported in Ref. 17 can also be applied to solve the approximate problem.

V. Optimization Procedure

An automated structural optimization system (ASOS) computer software has been developed to implement the optimization methodology. The GHC approximation, design variable linking, the optional accumulation of linearized constraints from previous iterations have been incorporated in ASOS. In addition, move limits, side constraints (limits placed on design variables), and general linear constraints have also been included in the program. ASOS has the capability of solving large structural optimization problems that may have as many as 10,000 static degrees of freedom, 500 normal modes of vibration, 200 design variables, and 20 frequency constraints. The ASOS program organization is shown in Fig. 1. It consists of five primary modules, i.e., the design data processor (DDP), normal modes analysis (NMA), design sensitivity analysis (DSA), approximate problem generator (APG), and optimizer.

MSC/NASTRAN is a large-scale, general-purpose digital computer code that solves a wide variety of engineering problems by the finite-element method.[18] This code is used

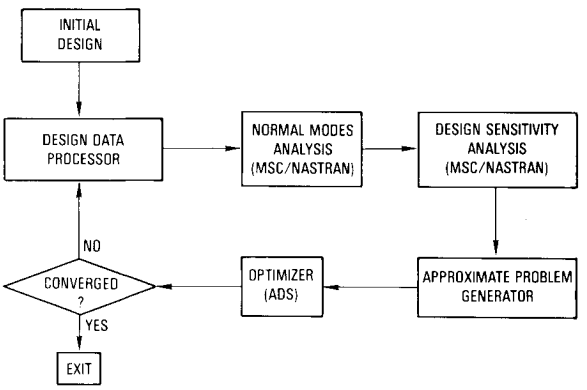

Fig. 1 ASOS program organization.

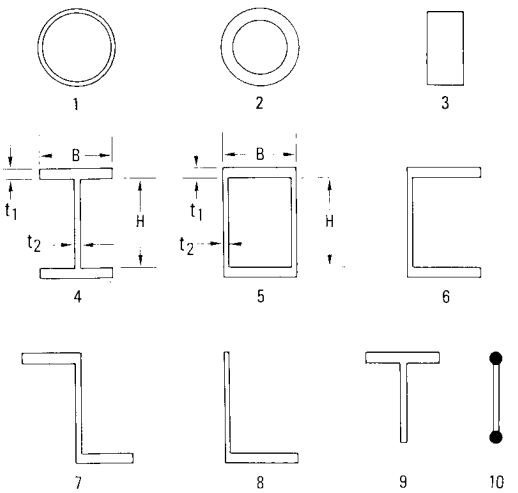

Fig. 2 Cross-sectional shapes in CSL.

to perform normal modes and design sensitivity analyses to obtain natural vibration frequencies, mode shapes, and eigenvalue derivatives required in the ASOS program. Many computer codes have been developed to implement optimization methods for NLP problems. A newly developed optimization program, ADS, described in Ref. 19, implements a large number of optimization algorithms for constrained and unconstrained problems. Although the computational experience to date is limited, the ADS code seems to have all the ingredients to become the premier tool in design optimization. Therefore, ADS is selected to be the optimizer in ASOS.

A library containing mathematical relations between cross-sectional properties and cross-sectional dimensions has been established. This library serves as an important link between the structural analysis and design because the required analysis input, such as the cross-sectional area and moment of inertia, can be found in the library for a given cross-sectional shape and a set of cross-sectional dimensions defined in the structural design. The cross-sectional library (CSL) contains ten cross-sectional shapes shown in Fig. 2. CSL can be used either as a submodule in the ASOS program or as an independent program for the computation of cross-sectional properties.

The interface task between the design and analysis is performed by the design data processor (DDP) of which CSL is a submodule. The design data and requirements, such as cross-sectional shapes and dimensions, the design variable linking scheme, and limits on frequencies and design variables are processed by DDP to generate data sets needed by other modules in ASOS. These data sets provide the section property input for the normal modes analysis and the definition of design variables and constraints for DSA and APG. Consistency between data sets is guaranteed because they are generated by DDP from the same data source.

The approximate problem generator incorporates various approximation techniques, including the GHC approximations and the optional linear approximate constraint accumulation. APG uses eigenvalues and their partial derivatives calculated by NMA and DSA to form an explicit approximate optimization problem for the optimizer. A number of control parameters in APG can be used to select an optimization algorithm in ADS, set the constraint accumulation tolerance, and adjust the values of p and n in the GHC approximation.

VI. Numerical Examples

The ASOS program has been applied to solve numerous large structural optimization problems in a practical engineering design-analysis environment. The results of three example problems are reported here to illustrate the efficiency of the optimization methodology. The method of feasible directions in the ADS code was used in all three example problems.

Problem 1: Cantilever Beam

The first example problem is the design optimization of a cantilever beam shown in Fig. 3. The beam is symmetric with respect to the midplane and supports three nonstructural masses. Web thicknesses (t_1,t_2,t_3) and chord areas (A_1,A_2,A_3) are determined so as to achieve a minimum structural weight while maintaining the fundamental frequency at or above 20

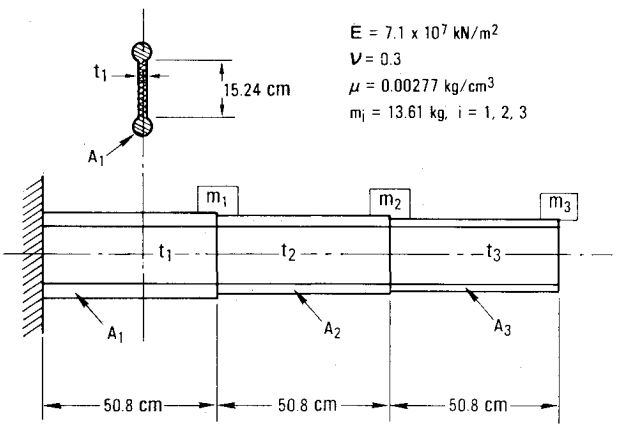

Fig. 3 Cantilever beam example problem.

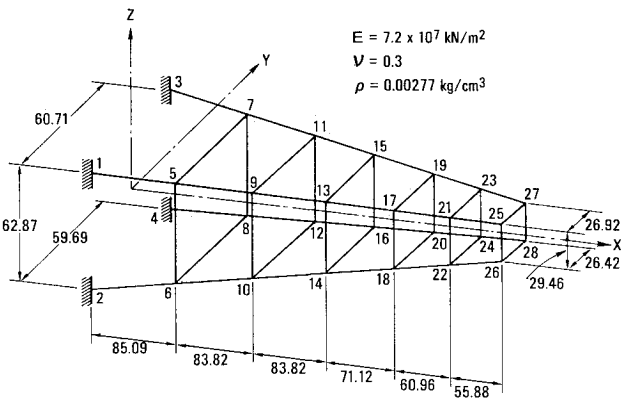

Fig. 4 Helicopter tail boom.

Table 1 Iteration history data for cantilever beam problem

Analysis no.	Structural weight, kg (frequency constraint violation, %)					
	Case 1A	Case 1B	Cases 1C and 1D	Case 1E	Case 1F	Case 1G
0	8.71 [0]	8.71 [0]	8.71 [0]	8.71 [0]	8.71 [0]	8.71 [0]
1	4.44 [2.3]	4.46 [2.2]	5.01 [0]	4.13	5.13 [0]	4.96 [0]
2	3.08 [7.7]	3.24 [5.5]	3.59 [0]	3.58	3.79 [0]	3.45 [0]
3	2.99 [3.9]	2.98 [5.1]	3.18 [0.3]	3.36	3.38 [0]	2.93 [0]
4	3.06 [3.1]	3.04 [6.6]	3.19 [0]	3.27	3.28 [0]	2.81 [0]
5	2.96 [6.2]	2.93 [5.4]	3.18 [0]	3.22	3.20 [0]	2.71 [0]
6	2.93 [4.8]	3.09 [2.7]	3.18 [0]	3.18	3.14 [0]	2.65 [0]
7	3.00 [12.3]	3.02 [3.1]	3.18 [0]	3.18 [0]	3.11 [0]	2.63 [0]
8	3.09 [3.6]	3.13 [1.2]			3.11 [0]	2.62 [0]
9	2.82 [9.0]	3.11 [1.9]			3.11 [0]	2.62 [0]
10	2.71 [11.0]	3.13 [2.0]				
11	3.03 [2.7]	3.14 [2.1]				
12	3.06 [2.8]	3.14 [1.2]				
13	2.98 [6.1]	3.15 [0.6]				
14	2.89 [5.1]	3.18 [0]				
15		3.18 [0]				

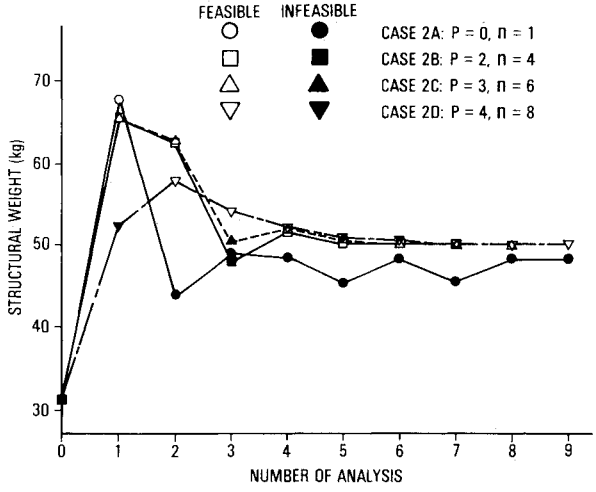

Fig. 5 Iteration history for helicopter tail boom problem.

Hz. No other constraints are imposed except for the small minimum gage restriction $A_i = 0.0645$ cm^2 and $t_i = 0.00254$ cm. For all cases, an initial design of $t_i = 0.508$ cm and $A_i = 6.45$ cm^2 is used.

Two distinct finite-element models are considered. One is made of truss and membrane elements, and the other consists of beam elements using cross-sectional shape number 10 in CSL. Optimization results obtained from the truss-membrane model using 50% move limits are shown in Table 1 for the following cases of frequency constraint approximations: case 1A) first-order Taylor series; case 1B) case 1A plus constraint accumulation; case 1C) GHC approximation with $p=0$, $n=1$; case 1D) case 1C plus constraint accumulation; and case 1E) results reported by Miura and Schmit in Ref. 9 using the second-order Taylor series.

The first-order Taylor series approximation of the frequency constraint in the design space is so poor that the design was driven into the infeasible region after one analysis, and it was unable to generate a feasible design after 14 complete finite-element analyses. Fifteen analyses were required in case 1B to obtain a near-optimum solution, which indicates that constraint accumulation is not an efficient method. Iteration histories for the structural weight in cases 1C and 1D are almost identical. A comparison between cases 1C and 1E indicates that the GHC approximation is much more efficient than the second-order Taylor series because it converges faster and is not burdened by the costly computation of the second-order eigenvalue derivatives.

The results of optimization using beam elements and 50% move limits are also shown in Table 1 for the following cases: case 1F) including shear deflection, GHC approximation with $p=0$, $n=1$; and case 1G) same as case 1F without shear deflection. Final designs and structural weights are listed in Table 2 for all cases with feasible final solutions. There is no significant difference between the results obtained in cases 1B–1E. The final designs and structural weight obtained for the beam models are quite different from those obtained for the truss-membrane model. The final structural weight for the beam model with shear deflection is 3.11 kg, which is slightly lower than the 3.18 kg for the truss-membrane model. The weight difference is not unexpected. The reason for the difference is that the web represented by membrane elements is more flexible than the web modeled by beam elements with shear deflection. For the same reason, the final weight of 2.62 kg obtained for the beam model without shear deflection is much smaller than that obtained for the other models. Therefore, modeling differences may have significant effects on the structural optimization results.

Table 2 Final designs for cantilever beam problem

Case	A_1, cm^2	A_2, cm^2	A_3, cm^2	t_1, cm	t_2, cm	t_3, cm	W, kg
1B	5.59	2.75	0.723	0.124	0.109	0.064	3.18
1C	5.59	2.85	0.703	0.117	0.104	0.064	3.18
1D	5.61	2.85	0.703	0.114	0.104	0.066	3.18
1E	5.62	2.85	0.697	0.112	0.102	0.066	3.18
1F	6.20	3.41	1.250	0.008	0.008	0.010	3.11
1G	5.30	2.83	0.871	0.015	0.015	0.013	2.62

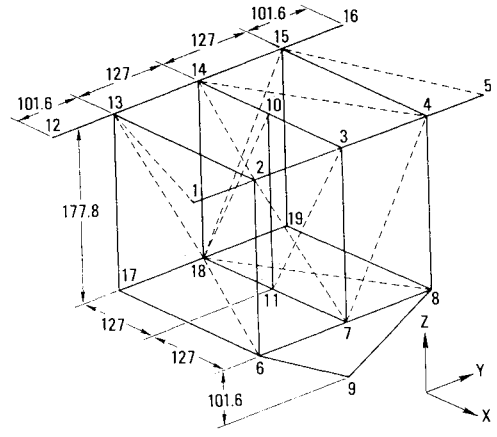

Fig. 6 Payload frame.

Problem 2: Helicopter Tail Boom

A space frame idealization of a helicopter tail boom is shown in Fig. 4 along with node numbers and dimensions given in centimeters. Element connectivities can be found in Table 2 of Ref. 20. The frame supports eight concentrated masses located at nodes 13, 14, 15, 16, 25, 26, 27, and 28. Each mass has a constant value of 22.68 kg. All members are made of thin-wall round tubes. The frame is designed for minimum weight subject to constraints placed on the fundamental frequency and R/t ratios (as preliminary measures against column and local wall buckling). The lower limit on the fundamental frequency is 10 Hz. The lower and upper limits on the R/t ratios are 10 and 40, respectively. The side constraints are $0.635 \le R \le 63.5$ cm and $0.00254 \le t \le 12.7$ cm for all members. The helicopter tail boom structural optimization problem was treated in Refs. 3 and 21 for constraints imposed on stresses, displacements, and R/t ratios.

The ASOS program was applied to solve this design problem. A total of four cases were investigated, and the GHC approximation was used in all cases: case 2A) $p=0$, $n=1$; case 2B) $p=2$, $n=4$; case 2C) $p=3$, $n=6$; and case 2D) $p=4$, $n=8$.

The initial design is the same for all cases, i.e., all members have an initial radius of 5.08 cm and a wall thickness of 0.13 cm. The fundamental frequency of the initial design is 6.75 Hz, which is 32.5% infeasible. Move limits of 50% are imposed in cases 2A, 2B, and 2C. In case 2D, the lower move limit is modified to be $1-(p-1) \div (p+1) = 0.4$ (40%) so that the GHC function is convex within the move limits and the feasible region of the approximate problem is also convex.

The iteration history of the structural weight is shown in Fig. 5. In case 2A, the GHC approximation of the frequency constraint with $p=0$ and $n=1$ is the same as the basic hybrid constraint approximation presented in Ref. 13. A heavy-weight feasible design was generated after the first normal modes analysis. From there on, the design stayed in the infeasible region, which indicates that the basic hybrid constraint is a poor approximation for this problem. The frequency constraint violation at the ninth analysis is 11.8%.

Table 3 Final designs for helicopter tail boom

Element no.	Design variable	Final design, cm Case 2b $p=2$, $n=4$	Case 2C $p=3$, $n=6$	Case 2D $p=4$, $n=8$
1-4	R	9.169	9.013	8.852
	t	0.220	0.228	0.224
5-8	R	3.845	4.455	5.008
	t	0.097	0.114	0.127
9-12	R	7.853	7.800	7.742
	t	0.197	0.197	0.197
13-16	R	6.471	6.424	6.477
	t	0.163	0.162	0.164
17-20	R	7.162	7.129	7.096
	t	0.179	0.180	0.180
21-24	R	5.895	5.920	6.035
	t	0.148	0.150	0.152
25-28	R	5.960	5.922	5.906
	t	0.149	0.151	0.149
29-32	R	5.247	5.277	5.363
	t	0.132	0.133	0.136
33-36	R	5.207	5.185	5.196
	t	0.131	0.133	0.132
37-40	R	5.168	5.169	5.274
	t	0.130	0.132	0.134
41-44	R	4.728	4.733	4.746
	t	0.119	0.119	0.120
45-48	R	4.037	4.067	4.142
	t	0.102	0.104	0.105

The GHC approximations in cases 2B, 2C, and 2D are more conservative than that in case 2A. The effects of constraint conservativeness are revealed by the optimization results displayed in Fig. 5. It can be seen that the structural weight trajectory during the early stages of the optimization process is more stable for cases in which the GHC approximation is more conservative. While the designs in cases 2B and 2C were driven into the infeasible region at the third analysis, the more conservative GHC in case 2D kept the design in the feasible region after two normal modes analyses were conducted. The final structural weight obtained in these three cases is approximately 50.35 kg, requiring seven to nine normal modes analyses.

The final designs for cases 2B, 2C, and 2D are given in Table 3. At the final design in each case, the frequency is at the lower bound of 10 Hz, and R/t ratios are at the upper bound of 40. The final design material distributions are almost the same for all three cases.

Problem 3: Payload Frame

The third example problem is the design of a payload frame structure that can be used in the Space Shuttle Orbiter to carry payloads. The finite-element model is shown in Fig. 6. Element connectivities in the model are given in Table 4. The dash lines in Fig. 6 represent circular tubes with hinged ends, and dimensions are given in centimeters. Elements 1-4 and 9-22 have cross-sectional shapes of rectangular boxes, and members 5-8 and 23-29 represent symmetric I beams. The frame is supported in the X and Z directions at nodes 1 and 5, in the Z direction at nodes 12 and 16, and in the Y direction at node 9. Material properties are identical to those used in the second example problem. The frame supports a total payload of 11,340 kg, represented by the concentrated masses in the finite-element model. The concentrated masses with a constant value of 907.2 kg are located at nodes 2, 4, 6, 8, 13, 15, 17, and 19, and those with a value of 680.4 kg are located at nodes 3, 7, 10, 11, 14, and 18. Lower limits are placed on the first three natural frequencies, i.e., $\omega_1 \geq 6$ Hz, $\omega_2 \geq 6.5$ Hz, and $\omega_3 \geq 9$ Hz. No other constraints are imposed except for small minimum gage restrictions $t \geq 0.00254$ cm and $A \geq 0.0645$ cm^2.

Table 4 Element connectivity for payload frame

Member	Node 1	Node 2	Member	Node 1	Node 2
1	1	2	22	8	9
2	4	5	23	10	14
3	2	3	24	3	10
4	3	4	25	11	18
5	12	13	26	7	11
6	15	16	27	14	18
7	13	14	28	10	11
8	14	15	29	3	7
9	2	13	30	1	13
10	4	15	31	5	15
11	2	6	32	2	14
12	4	8	33	4	14
13	6	17	34	6	18
14	8	19	35	8	18
15	13	17	36	2	7
16	15	19	37	4	7
17	6	7	38	13	18
18	7	8	39	15	18
19	17	18	40	10	18
20	18	19	41	3	11
21	6	9			

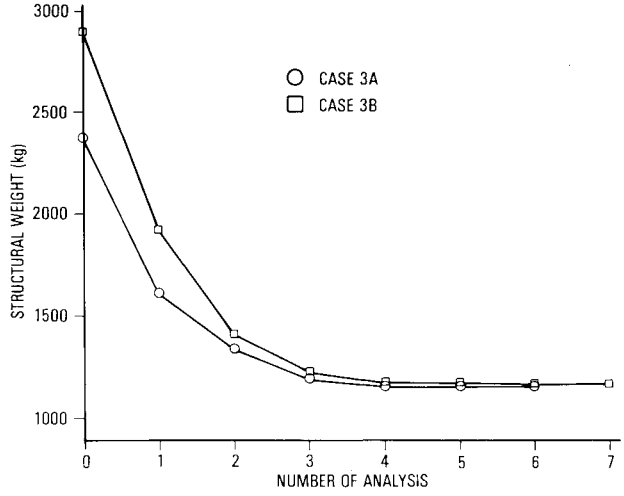

Fig. 7 Iteration history for payload frame problem.

The problem was solved by ASOS using the GHC approximation with $p=0$, $n=1$, and 50% move limits. The following two cases were studied: case 3A) the initial design has a thickness of 2.54 cm for all elements with box or I cross sections and a cross-sectional area of 64.5 cm^2 for members with hinged ends; case 3B) the initial design is $t_1 = 5.08$ cm and $t_2 = 1.27$ cm for members with box or I cross sections ($A = 129$ cm^2 for elements 30, 31, 34, 35, 38, 39, and 41; $A = 32.25$ cm^2 for elements 32, 33, 36, 37, and 40).

The iteration history for the structural weight is displayed in Fig. 7. The design in both cases stayed in the feasible region during the entire optimization process. The final structural weights are 1173 and 1183 kg for cases 3A and 3B, respectively. The final designs are given in Table 5. The material distribution of the final design in case 3A is significantly different from that in case 3B. While the third natural frequency constraint is critical in case 3A, the second frequency is at the lower limit in case 3B. The third vibration mode in case 3A is a local mode in which nodes 10 and 11 move out of the XZ plane and the rest of the frame is almost stationary. The second mode in case 3B is a global vibration mode in which the members move primarily in the x direction and rotate about the Y axis. It is obvious that this structural optimization problem possesses multiple local optima.

Table 5 Final designs for payload frame

Element no.	Cross section			Final design			
				Case 3A		Case 3B	
	Shape	B, cm	H, cm	t_1, cm	t_2, cm	t_1, cm	t_2, cm
1,2	Box	20.32 (X)[a]	35.56	1.743	0.901	1.895	0.748
3,4	Box	20.32 (X)	35.56	1.716	0.853	1.585	0.672
5,6	I	15.24 (X)	30.48	2.190	1.602	2.143	0.985
7,8	I	15.24 (X)	30.48	2.047	1.470	1.821	0.929
9,10	Box	12.70 (Y)	12.70	1.037	0.961	1.230	0.781
11,12		12.70 (Y)	12.70	1.277	1.231	1.673	0.910
13,14		12.70 (Y)	12.70	0.918	0.830	1.215	0.775
15,16		12.70 (Y)	12.70	1.251	1.232	1.618	0.888
17,18		12.70 (X)	20.32	1.391	1.000	2.093	0.850
19,20		12.70 (X)	20.32	1.384	0.979	2.073	0.845
21,22	Box	10.16 (X)	20.32	1.338	0.820	2.080	0.775
23,24	I	10.16 (Y)	25.40	1.748	1.392	2.485	0.975
25,26		10.16 (Y)	25.40	1.620	1.328	2.454	0.975
27		10.16 (Y)	15.24	1.820	1.961	2.931	1.132
28		10.16 (Y)	15.24	1.779	1.914	2.926	1.132
29	I	10.16 (Y)	15.24	1.884	2.008	2.939	1.133
30,31		Truss member[b]		$A=30.79$		$A=30.03$	
32,33				$A=25.19$		$A=19.60$	
34,35				$A=19.56$		$A=27.56$	
36,37				$A=35.15$		$A=23.99$	
38,39				$A=34.92$		$A=33.63$	
40				$A=41.14$		$A=25.63$	
41		Truss member		$A=39.59$		$A=58.41$	

[a]Letter within parentheses indicates the direction along which B is measured. [b]Cross-sectional areas in square centimeters are listed for truss members.

VII. Concluding Remarks

A structural optimization methodology has been presented herein for the design of three-dimensional space frames subject to multiple frequency constraints. The methodology has been implemented in a general-purpose, large-scale computer code ASOS that has been used to solve a variety of practical structural optimization problems. The numerical results of the example problems described here illustrate the efficiency of the ASOS program. The difficulty caused by the inherent nonlinearity of the frequency constraint has been overcome and a near-optimum solution can usually be obtained by ASOS, requiring only five to 10 complete normal modes analyses.

The generalized hybrid constraint has been developed to provide a class of powerful constraint approximations whose conservativeness can be tuned by adjusting the values used for a set of parameters. The GHC functions are separable functions of the independent design variables. Proof is given in this paper that a very useful subclass of the GHC functions is convex in the region bounded by move limits. The formula for calculating these move limits is also presented here so that the approximate problems generated in the optimization process are theoretically guaranteed to be separable and convex. As a consequence, both the primal and dual mathematical programming methods can be applied to obtain a global optimum solution for the approximate problem. Although the GHC approximation has been developed for the frequency constraint and the frame-type structure, it can be applied to other types of constraints and structures encountered in structural optimization problems.

For a structural optimization tool to be useful in an engineering design environment, it must be user-friendly and capable of solving practical structural design problems. The powerful GHC approximation has made it possible that only a standard set of approximation concepts are required in the ASOS program without any loss in efficiency. Users of ASOS do not have to face the difficult and sometimes agonizing decision-making process of selecting the proper type of design variables and constraint approximations. A comprehensive cross-sectional library, approximation techniques, and the generality of MSC/NASTRAN and ADS have made the ASOS program capable of solving practical design optimization problems for a large class of three-dimensional space frame structures.

Acknowledgments

The author would like to thank Professor Lucien Schmit of UCLA for many helpful discussions and suggestions, and Messrs. Bob Van Vooren and Sesto Voce of TRW for their encouragement and support. This work was supported by TRW Independent Research and Development, Project 85330125.

References

[1]Mills-Curran, W. C., Lust, R. V., and Schmit, L. A., "Approximation Methods for Space Frame Synthesis," *AIAA Journal*, Vol. 21, Nov. 1983, pp. 1571-1580.

[2]Khan, M. R., Thornton, W. A., and Willmert, K. D., "Optimization of Structures with Multiple Design Variables per Member," *AIAA Journal*, Vol. 20, Sept. 1982, pp. 1282-1283.

[3]Lust, R. V. and Schmit, L. A., "Alternative Approximation Concepts for Space Frame Synthesis," *AIAA Journal*, Vol. 24, Oct. 1986, pp. 1676-1684.

[4]Yoshida, N. and Vanderplaats, G. N., "Structural Optimization Using Beam Elements," *paper presented at the AIAA/ASME/ASCE/AHS 26th Structures, Structural Dynamics and Materials Conference*, Orlando, FL, April 1985.

[5]Turner, M. J., "Design of Minimum Mass Structures with Specified Natural Frequencies," *AIAA Journal*, Vol. 5, March 1967, pp. 406-412.

[6]Prager, W. and Taylor, J. E., "Problems of Optimal Structural Design," *Journal of Applied Mechanics*, Vol. 35, March 1968, pp. 102-106.

[7]Rubin, C. P., "Minimum Weight Design of Complex Structures Subject to a Frequency Constraint," *AIAA Journal*, Vol. 8, May 1970, pp. 923-927.

[8]Sippel, D. L. and Warner, W. H., "Minimum-Mass Design of Multielement Structures Under a Frequency Constraint," *AIAA Journal*, Vol. 11, April 1973, pp. 483-488.

[9]Miura, H. and Schmit, L. A., "Second Order Approximation of Natural Frequency Constraints in Structural Synthesis," *International Journal of Numerical Methods in Engineering*, Vol. 13, 1978, pp. 337-351.

[10]Schmit, L. A. and Farshi, B., "Some Approximation Concepts for Structural Synthesis," *AIAA Journal*, Vol. 12, May 1974, pp. 692-699.

[11]Fox, R. L. and Kapoor, M. D., "Rates of Change of Eigenvalues and Eigenvectors," *AIAA Journal*, Vol. 6, Dec. 1968, pp. 2426-2429.

[12]Nelson, R. B., "Simplified Calculation of Eigenvector Derivatives," *AIAA Journal*, Vol. 14, Sept. 1976, pp. 1201-1205.

[13]Starnes, J. H. Jr. and Haftka, R. T., "Preliminary Design of Composite Wings for Buckling, Stress and Displacement Constraints," *Journal of Aircraft*, Vol. 16, Aug. 1979, pp. 564-570.

[14]Prasad, B., "Novel Concepts for Constraint Treatments and Approximations in Efficient Structural Synthesis," *AIAA Journal*, Vol. 22, July 1984, pp. 957-966.

[15]Prasad, B., "Explicit Constraint Approximation in Structural Optimization—Part 1: Analyses and Projections," *Computer Methods in Applied Mechanics and Engineering*, Vol. 40, Sept. 1983, pp. 1-26.

[16]Woo, T. H. and Schmit, L. A., "Decomposition in Optimal Plastic Design of Structures," *International Journal of Solids and Structures*, Vol. 17, No. 1, Jan. 1981, pp. 39-56.

[17]Fleury, C. and Schmit, L. A., "Dual Methods and Approximation Concepts in Structural Synthesis," NASA 3226, Dec. 1980.

[18]*MSC/NASTRAN User's Manual*, edited by C. W. McCormick, The MacNeal-Schwendler Corp., MSR39, 1983.

[19]Vanderplaats, G. N., "ADS—A FORTRAN Program for Automated Design Synthesis—Version 1.00," NASA 172460, Oct. 1984.

[20]Woo, T. H., "Space Frame Optimization Subject to Frequency Constraints," *Proceedings of AIAA/ASME/ASCE/AHS 27th Structures, Structural Dynamics and Materials Conference*, San Antonio, TX, May 1986, pp. 103-115.

[21]Govil, A. K., Arora, J. S., and Haug, E. J., "Optimal Design of Frames with Substructuring," *Computers and Structures*, Vol. 12, 1980, pp. 1-10.

Errata

Initial Instability in a Freejet Mixing Layer Measured by Laser Doppler Anemometry

S. Einav, J. M. Avidor, and E. Gutmark
Tel Aviv University, Israel
and
M. Gaster
National Maritime Institute, Teddington, England

[AIAAJ 25, No. 4, pp. 628-630 (1987)]

The captions for Figures 3 and 5 were transposed.